Thermal effects in plasma-based accelerators[a)]

E. Esarey,[1,2,b)] C. B. Schroeder,[1] E. Cormier-Michel,[2] B. A. Shadwick,[3,1] C. G. R. Geddes,[1] and W. P. Leemans[1,2]
[1]*Lawrence Berkeley National Laboratory, Berkeley, California 94720*
[2]*Department of Physics, University of Nevada, Reno, Nevada 89557*
[3]*Institute for Advanced Physics, Conifer, Colorado 80433*

(Received 3 November 2006; accepted 13 February 2007; published online 1 May 2007)

Finite plasma temperature can modify the structure of the wake field, reduce the wave-breaking field, and lead to self-trapped electrons, which can degrade the electron bunch quality in a plasma-based accelerator. A relativistic warm fluid theory is used to describe the plasma temperature evolution and alterations to the structure of a nonlinear periodic wave exited in a warm plasma. The trapping threshold for a plasma electron and the fraction of electrons trapped from a thermal distribution are examined using a single-particle model. Numerical artifacts in particle-in-cell models that can mimic the physics associated with finite momentum spread are discussed. © *2007 American Institute of Physics*. [DOI: 10.1063/1.2714022]

I. INTRODUCTION

Plasma-based accelerators are capable of supporting large amplitude plasma waves with electric fields up to hundreds of GV/m, approximately three orders of magnitude beyond conventional accelerators.[1] Previously, laser-plasma accelerator experiments[2–7] have typically operated in the self-modulated regime of the laser wake field accelerator (LWFA). In this regime, a long (compared to the plasma wavelength), high-power laser pulse drives a plasma wave through a Raman or self-modulation instability. The plasma wave amplitude grows exponentially inside the laser pulse, via the instability, until the growth saturates nonlinearly or electrons become trapped in the plasma wave (subsequently damping the plasma wave due to beam loading). Experimentally and numerically, significant electron trapping is found to occur when the plasma wave amplitude surpasses a critical threshold, often loosely referred to as wave breaking.[2,7–9] Uncontrolled trapping can result in the production of electron beams with near 100% energy spread, which limits the application of these beams.

More recently, near-monoenergetic electron bunches have been produced in laser-plasma accelerator experiments in the 100-MeV range,[8–10] as well as the 1-GeV range.[11] The source of the accelerated electrons was self-trapping from the background plasma. Narrow energy spread electron beams were produced through control of the interaction length such that the acceleration occurred over a dephasing length.[12]

To further improve the electron bunch quality and stability, a variety of laser-triggered injection methods have been proposed,[13–17] and controlled injection via colliding laser pulses has been achieved experimentally.[18] The next generation of plasma accelerator experiments is likely to use a two-stage approach. The first stage would be a relatively low-energy injector, wherein the accelerated electron bunch is produced through self-trapping or laser-triggered injection. The electron bunch would then be injected into the second stage, which would be a "dark current free" structure that would accelerate the bunch to high energy. A dark current free structure refers to the structure not generating any additional accelerated electrons through any self-trapping process. In order to assess the viability of present and future plasma accelerator experiments, a detailed understanding and control of self-trapping are essential.

Traditionally, fluid theories have been used to define and analyze wave breaking (the maximum plasma wave amplitude of a nonlinear traveling wave).[19–24] Previous hydrodynamic wave-breaking theories in one dimension have been carried out for plasmas in the cold limit,[19] warm plasmas in the nonrelativistic limit,[21] and warm plasmas in the limit of ultrarelativistic phase velocities.[22,23] The cold, relativistic wave-breaking field[19] is $\sqrt{2}(\gamma_\varphi-1)^{1/2}E_0$, where $\gamma_\varphi^2=1/(1-\beta_\varphi^2)$, $v_\varphi=c\beta_\varphi$ is the plasma wave phase velocity (approximately the group velocity of the driver), $E_0=cm\omega_p/e$, $\omega_p=ck_p=(4\pi n_0 e^2/m)^{1/2}$ is the plasma frequency, and n_0 is the ambient electron plasma density. When the plasma wave field approaches $\sqrt{2}(\gamma_\varphi-1)^{1/2}E_0$, the cold plasma density becomes singular,[20] indicating a breakdown of the cold fluid model. In the ultrarelativistic phase velocity $\beta_\varphi=1$ limit, the warm wave-breaking field was found[22,23] to be $E_{\rm th}\sim\theta^{-1/4}E_0$, where θ is the initial plasma temperature normalized to $mc^2/k_{\rm B}$, with $k_{\rm B}$ the Boltzmann constant. This expression for $E_{\rm th}$ is valid for $\gamma_\varphi\theta^{1/2}\gg 1$, e.g., for an ultrarelativistic ($\beta_\varphi=1$) particle beam driver. For laser-driven plasma waves, however, typically plasma wave phase velocities are $\gamma_\varphi\sim 10$–100 and initial plasma temperatures are $\theta mc^2\sim 10$ eV (Refs. 25 and 26). Therefore, a laser-plasma accelerator typically satisfies $\gamma_\varphi\theta^{1/2}<1$ and, hence, the above expression for $E_{\rm th}$ does not apply. Recently, a warm, relativistic fluid theory has been used to describe wave breaking in the regime of interest to laser-plasma accelerators.[24]

For electric-field amplitudes below the wave-breaking field, significant electron trapping may occur in a warm plasma. In a warm plasma, such as that characterized by a Gaussian distribution, fast electrons may exist on the tail of

[a)]Paper UI2 3, Bull. Am. Phys. Soc. **51**, 259 (2006).
[b)]Invited speaker.

the distribution that can have sufficiently high momenta to allow trapping in the plasma wave. Using a test particle trapping formalism, the threshold momentum for an electron to become trapped in a plasma wave with an amplitude below the wave-breaking limit can be calculated.[27] Consequently, the fraction of electrons trapped from the tail of the distribution, which constitutes the dark current, can be determined.[27] Furthermore, the amount of trapping at the hydrodynamic warm wave-breaking limit can also be determined.

In this paper, some consequences of finite temperature on plasma-based accelerators are discussed. In Sec. II, the results of a warm, relativistic fluid model are presented. This model describes the evolution of the temperature in a plasma wake field, as well as modification of the wake field due to finite temperature. The warm wave-breaking limit for nonrelativistic plasma temperatures is presented. Section III discusses trapping and dark current with a test particle model. Section IV discusses numerical heating and subsequent trapping when modeling plasma accelerators with particle-in-cell codes. Conclusions are given in Sec. V.

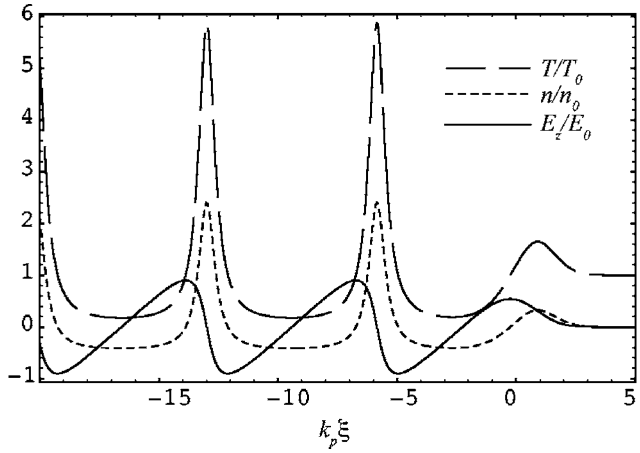

FIG. 1. Plasma density n/n_0 (dotted curve), plasma wave electric field E_z/E_0 (solid curve), and plasma temperature T/T_0 (dashed curve) excited by a Gaussian laser pulse with normalized intensity $a=2$ and RMS length $k_pL_{\mathrm{RMS}}=1$ (centered at $k_p\xi=0$).

II. WARM WAVE BREAKING

Standard warm relativistic fluid theories derived for collisionally dominated plasmas (e.g., Ref. 28) are inadequate for describing short-pulse laser-plasma interactions. Short-pulse laser-plasma interactions access a collisionless regime that is not in local thermodynamical equilibrium, in which the plasma electrons experience relativistic motion while the temperature (electron momentum spread) remains small. To model short-pulse laser-plasma interactions, a warm relativistic fluid model can be derived from the collisionless Boltzmann equation.[24,29] By assuming that the plasma is "warm," such that the phase-space distribution has a small momentum spread about its mean, allows the hierarchy of moment equations to be treated asymptotically.[29–33] No additional assumptions concerning the specific form of the distribution are required for closure of the fluid equations. Assuming the quasistatic approximation,[34] i.e., the plasma wave driver and fluid quantities are assumed to be functions only of the comoving variable $\xi=z-\beta_\varphi ct$ (where z is the driver propagation direction), the fluid equations can be combined to yield the evolution equation for the nonlinear one-dimensional (1D) plasma response,[24]

$$\frac{\partial^2}{\partial\xi^2}\left[\frac{\gamma_\perp(1-\beta_\varphi w_z)}{(1-w_z^2)^{1/2}}+\frac{3}{2}\theta\frac{(1-\beta_\varphi w_z)(1-w_z^2)^{1/2}}{\gamma_\perp(1-\beta_\varphi^{-1}w_z)^2}\right]=\frac{k_p^2w_z}{\beta_\varphi-w_z}, \tag{1}$$

where $\theta=k_BT_0/mc^2$ is the initial isotropic temperature, $\gamma_\perp^2=1+a^2/2$, $a^2\simeq 7.3\times10^{-19}\lambda_0^2[\mu\mathrm{m}]I_0[\mathrm{W/cm^2}]$ is the normalized laser intensity for a linear polarized laser pulse, λ_0 is the laser wavelength, and I_0 is the laser intensity. Here w_z is the axial component of the fluid velocity given by $\mathbf{w}=(\int d\Omega f\mathbf{p})/(\int d\Omega f\gamma)$, where f is the phase-space density, $\mathbf{p}=\gamma\boldsymbol{\beta}$ is the normalized particle momentum, and $d\Omega=d\mathbf{p}/\gamma$ is the invariant momentum space volume element. Linearizing Eq. (1) yields the driven wave equation $[\partial_\xi^2+k_p^2(1+3\theta/2)]w_z=\partial_\xi^2a^2$, for a plasma wave with relativistic phase velocity ($\beta_\varphi\simeq1$). In the linear regime $a^2\ll1$, the dominant thermal effect is a change in the wavelength of the 1D plasma wave $\lambda_{\mathrm{osc}}\simeq\lambda_p(1-3\theta/4)$.

In terms of the axial fluid velocity, the plasma density is $n/n_0=w_z/(\beta_\varphi-w_z)$, the electrostatic potential (normalized to mc^2/e) is

$$\phi=\frac{\gamma_\perp(1-\beta_\varphi w_z)}{(1-w_z^2)^{1/2}}+\frac{3}{2}\theta\frac{(1-\beta_\varphi w_z)(1-w_z^2)^{1/2}}{\gamma_\perp(1-\beta_\varphi^{-1}w_z)^2}-1-\frac{3}{2}\theta, \tag{2}$$

the electric field is $E_z/E_0=-k_p^{-1}\partial_\xi\phi(w_z)$, and $k_BT/mc^2=(1-w_z^2)(1-\beta_\varphi^{-1}w_z)^{-2}\theta$ is the plasma temperature [measure of thermal spread given by the contraction of the momentum variance tensor, $k_BT/mc^2=\mathcal{U}^\mu\mathcal{U}_\mu-1$, with the hydrodynamic four momentum given by $\mathcal{U}^\mu=(\int d\Omega fp^\mu)/(\int d\Omega f)$] (Ref. 24). The warm fluid approximation assumes $k_BT/mc^2<1$ (i.e., nonrelativistic temperatures). Figure 1 shows the plasma density n/n_0 (dotted curve), plasma wave electric field E_z/E_0 (solid curve), and plasma temperature T/T_0 (dashed curve) excited by a Gaussian laser pulse $a=a_0\exp(-\xi^2/4L_{\mathrm{RMS}}^2)$ with normalized peak intensity $a_0=2$ and intensity RMS length $k_pL_{\mathrm{RMS}}=1$. The plasma temperature undergoes periodic oscillations in the wake owing to compression of the plasma density.[29] Note that the temperature evolution (to lowest order in the small parameter $k_BT/mc^2<1$) is given by $T=[(n/n_0)^2(1-w_z^2)]T_0$. The temperature evolution can be evaluated using the warm plasma approximation and does not require the choice of a specific distribution, in contrast to the claims of Ref. 35.

The warm fluid model can be used to determine the maximum field amplitude $\hat{E}_{\max}=E_{\max}/E_0$ of a nonlinear periodic plasma wave with phase velocity β_φ excited in a plasma with initial temperature θ, i.e., the warm wave-breaking field,[24]

$$\hat{E}_{\max}^2 = \gamma_\perp(\chi_0+\chi_0^{-1}-2) + \left\{\frac{6\beta_\varphi^2\chi_0[(1-\chi_0^4)-\beta_\varphi(\chi_0^4-2\chi_0^2/3+1)]}{[(1-\beta_\varphi)-(1+\beta_\varphi)\chi_0^2]^3}-1\right\}\frac{\theta}{\gamma_\perp}, \quad (3)$$

where

$$\chi_0^2 = \gamma_\varphi^2(1-\beta_\varphi)^2+\frac{1}{2}\gamma_\perp^{-2}(1+\beta_\varphi)^{-2}\{3\beta_\varphi^2\theta+\beta_\varphi(48\theta\gamma_\perp^2/\gamma_\varphi^2 + 9\beta_\varphi^2\theta^2)^{1/2}+[6\theta\beta_\varphi^2(10\gamma_\perp^2/\gamma_\varphi^2+3\beta_\varphi^2\theta) + 2\beta_\varphi(2\gamma_\perp^2/\gamma_\varphi^2+3\beta_\varphi^2\theta)(48\theta\gamma_\perp^2/\gamma_\varphi^2+9\beta_\varphi^2\theta^2)^{1/2}]^{1/2}\}. \quad (4)$$

Here $\chi_0=(1-w_z)/(1-w_z^2)^{1/2}$ is the extrema of the fluid momentum in the comoving frame. The maximum density perturbation is given by $(n/n_0)_{\max}=[1-\beta_\varphi^{-1}(1-\chi_0^2)/(1+\chi_0^2)]^{-1}$, which does not become singular in contrast to the cold fluid theories[19,20] (i.e., there is no shock formation). Furthermore, the absence of a singularity indicates that the fluid model remains valid, i.e., there is no breakdown of the fluid model at (or before) the wave-breaking limit (contrary to the claims of Ref. 35). For wave amplitudes larger than Eq. (3), no traveling wave solutions to the fluid equations exist. At the warm hydrodynamic wave-breaking limit, the amplitude of the force due to thermal pressure and the space-charge force are equal. The peak plasma temperature at the maximum plasma wave amplitude occurs at the point of maximum compression and is given by $(k_BT/mc^2)_{\max}=4\theta\chi_0^2[(1+\chi_0^2)-\beta_\varphi^{-1}(1-\chi_0^2)]^{-2}$. For a typical laser-plasma accelerator experiment, $\gamma_\varphi\sim 10$–100, $\gamma_\perp\sim 1$, and $\theta mc^2\sim 10$ eV (Refs. 25 and 26). In this regime $\theta\ll\gamma_\perp^2/\gamma_\varphi^2\ll 1$, and the maximum temperature to leading order is $(k_BT/mc^2)_{\max}\simeq\gamma_\perp(\gamma_\varphi^2\theta/3)^{1/2}[1-(3\gamma_\varphi^2\theta/3)^{1/2}/(4\gamma_\perp)]\ll 1$, which confirms the validity of the warm plasma approximation at the maximum plasma wave amplitude.

If the temperature becomes relativistic, the asymptotic expansion used above will no longer be valid. For relativistic temperatures, the higher-order moments of the distribution will be important and will be a function of the specific form of the phase-space distribution. Note that choice of an unphysical distribution (e.g., water bag) may lead to singular (unbounded) solutions. These singularities are not physical (as speculated in Ref. 35), but the result of the choice of an unphysical phase-space distribution. It should also be noted that for sufficiently large (or singular) density, the collisionless plasma model will no longer be valid.

In the cold plasma limit ($\theta=0$), Eq. (3) reduces to $\hat{E}_{\max}^2(\theta=0)=2\gamma_\perp(\gamma_\varphi-1)$. This is a generalization[24,27] of the cold relativistic wave-breaking field[19,36] to include the presence of a laser field. In the regime relevant to laser-plasma accelerator experiments, $\theta\ll\gamma_\perp^2/\gamma_\varphi^2\ll 1$, Eq. (3) reduces to[24]

$$\hat{E}_{\max}^2 \simeq 2\gamma_\perp(\gamma_\varphi-1)-\gamma_\varphi\left[\frac{8}{3}(3\gamma_\varphi^2\gamma_\perp^2\theta)^{1/4}-2(3\gamma_\varphi^2\theta)^{1/2}\right]. \quad (5)$$

Equation (5) is the cold relativistic wave-breaking field with the lowest-order reduction due to the plasma temperature. For high-intensity lasers ($a^2\gtrsim 1$), Eq. (5) indicates that $E_{\max}$ inside a laser pulse is significantly larger compared to behind the pulse (where $a=0$) (Ref. 24).

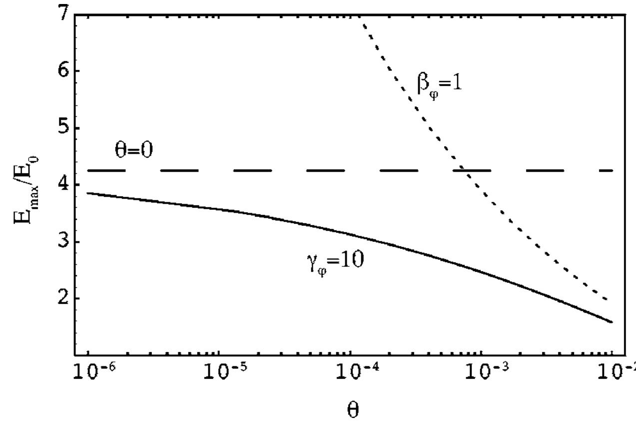

FIG. 2. Maximum plasma wave electric-field amplitude $\hat{E}_{\max}=E_{\max}/E_0$ [Eq. (3)] vs initial temperature θ with $\gamma_\varphi=10$ and $\gamma_\perp=1$. The dotted curve is the ultrarelativistic result $\beta_\varphi=1$, and the dashed line is the cold limit.

Figure 2 shows the wave-breaking field, Eq. (3), $\hat{E}_{\max}=E_{\max}/E_0$ (solid curve) versus initial temperature θ with $\gamma_\varphi=10$ and $\gamma_\perp=1$. The dotted curve is the ultrarelativistic result ($\beta_\varphi=1$), and the dashed line is the cold limit ($\theta=0$). Note that for typical short-pulse laser-plasma-interactions, $\theta\sim 10^{-4}$. Figure 3(a) shows the peak density perturbation calculated by solving Eq. (1) assuming a drive laser pulse with a Gaussian longitudinal profile $a=a_0\exp(-\xi^2/4L_{\mathrm{RMS}}^2)$ with a RMS intensity pulse length of $k_pL_{\mathrm{RMS}}=1$ propagating in a plasma with density such that $\gamma_\varphi=10$. As the amplitude approaches the wave-breaking limit $(\delta n/n_0)_{\max}=[1-\beta_\varphi^{-1}(1-\chi_0^2)/(1+\chi_0^2)]^{-1}-1$ (dotted line), the peak density perturbation is modified from the cold result. Figure 3(b) shows the difference between the nonlinear plasma wavelengths $(\Delta\lambda/\lambda_p)/\theta=[\lambda_{\mathrm{osc}}(\theta=0)-\lambda_{\mathrm{osc}}]/(\theta\lambda_p)$ (solid curve), the peak electric fields $(\Delta E/E_0)/\theta=[E_z(\theta=0)-E_z]/(\theta E_0)$ (dotted curve), and the peak electrostatic potentials $\Delta\phi/\theta=[\phi(\theta=0)-\phi]/\theta$ (dashed curve), assuming an initially cold ($\theta=0$) and warm ($\theta=10^{-3}$) plasma versus drive laser amplitude a_0 (with $k_pL_{\mathrm{RMS}}=1$ and $\gamma_\varphi=10$). Note that the differences plotted in Fig. 3(b) are normalized by θ. As Fig. 3(b) indicates, the normalized potential and electric field of the wave in a warm plasma differ from the cold result by a factor of order $\sim\theta\ll 1$ (typically $\theta\sim 10^{-4}$), and below wave breaking, the electric field is well modeled by the cold plasma result for nonrelativistic initial temperatures.[29] This refutes the claims of Ref. 35 that the cold plasma response cannot be used to approximately model the electrostatic field of a plasma wave below wave breaking. For $a_0\ll 1$, $[\lambda_{\mathrm{osc}}(\theta=0)-\lambda_{\mathrm{osc}}]/(\theta\lambda_p)=3/4$ (the 1D relativistic Bohm-Gross thermal shift in the plasma wavelength), as shown in Fig. 3(b).

III. PARTICLE TRAPPING

The dynamics of an electron in the presence of a plasma wave and a laser pulse is determined by the Hamiltonian in the comoving frame,[37] $H=(\gamma_\perp^2+u^2)^{1/2}-\beta_\varphi u-\phi(\xi)$, where u is the electron momentum normalized to mc. Assuming the

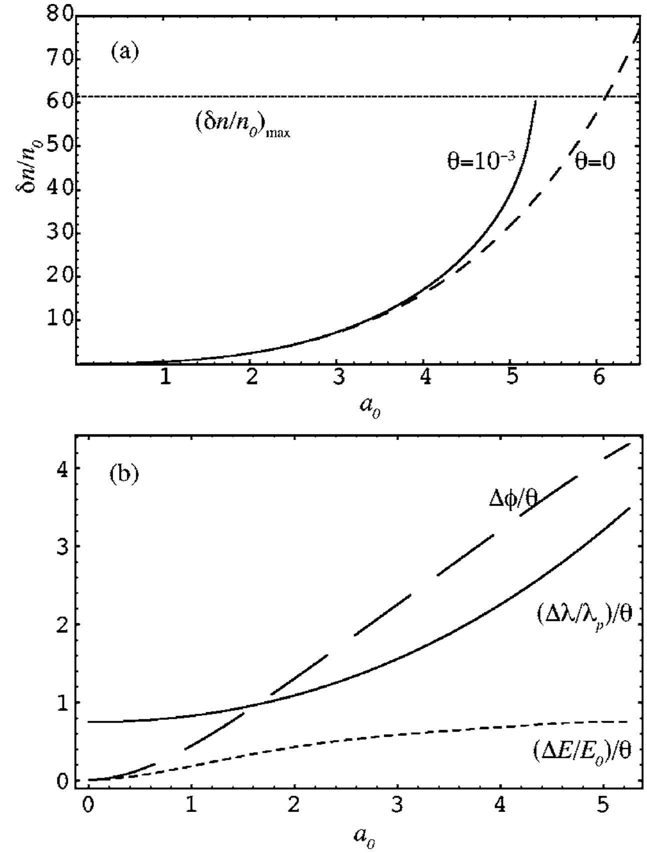

FIG. 3. (a) Peak density perturbation vs amplitude of drive laser a_0 (with $k_p L_{\mathrm{RMS}}=1$ and $\gamma_\varphi=10$) for initial plasma temperature of $\theta=10^{-3}$ (solid curve) and $\theta=0$ (dashed curve). The dotted line in (a) is the wave-breaking limit $(n/n_0)_{\max}-1$ behind the drive laser for $\gamma_\varphi=10$ and $\theta=10^{-3}$. (b) Differences between the nonlinear plasma wavelengths $(\Delta\lambda/\lambda_p/\theta)$ (solid curve), between the peak electric field amplitudes $(\Delta E/E_0)/\theta$ (dotted curve), and between the peak potential amplitudes $\Delta\phi/\theta$ (dashed curve), assuming an initially cold ($\theta=0$) and warm ($\theta=10^{-3}$) plasma vs drive laser amplitude a_0.

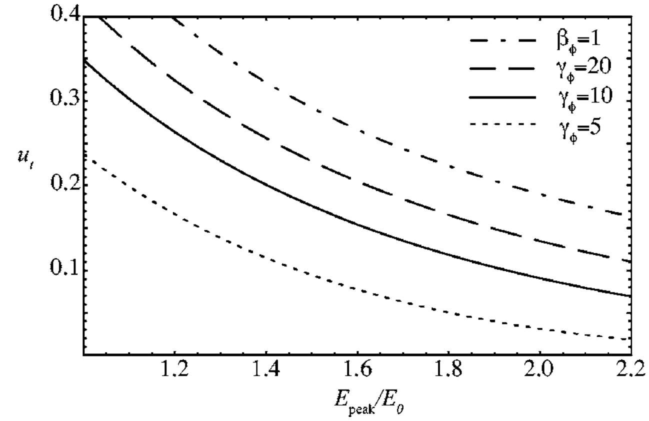

FIG. 4. Initial electron momentum u_t required to be trapped by a plasma wave with field amplitude E_{peak}/E_0 and phase velocity $\gamma_\varphi=5$ (dotted curve), $\gamma_\varphi=10$ (solid curve), $\gamma_\varphi=20$ (dashed curve), and $\beta_\varphi=1$ (dash-dotted curve), assuming an initial plasma temperature $\theta=10^{-4}$.

quasistatic approximation, the Hamiltonian is time independent and, therefore, a constant of motion $H(u,\xi)=$constant. The electron momentum at any phase is

$$u=\beta_\varphi\gamma_\varphi^2(H+\phi)\pm\gamma_\varphi[\gamma_\varphi^2(H+\phi)^2-\gamma_\perp^2]^{1/2}. \tag{6}$$

Equation (6) describes trapped (closed) and untrapped (open) orbits, in which a particular orbit is specified by a particular value of $H=$constant. The separatrix orbit between trapped and untrapped orbits is given by $H=H_s$, where $H_s=\gamma_\perp(\xi_m)/\gamma_\varphi-\phi(\xi_m)$. Here, ξ_m is the phase that maximizes $H(\gamma_\perp(\xi)\gamma_\varphi\beta_\varphi,\xi)$. Assuming $\gamma_\perp=$constant, $\phi(\xi_m)=\phi_{\min}$ is the minimum potential of the plasma wave.

Consider a plasma electron with initial normalized momentum u_t in the absence of any fields (i.e., before the passage of the driver and excitation of the plasma wave, $\gamma_\perp=1$ and $\phi=0$). The orbit of the electron will be defined by the Hamiltonian $H=H_t$, where $H_t=(1+u_t^2)^{1/2}-\beta_\varphi u_t$. Trapping of the electron will occur when the orbit defined by the Hamiltonian H_t coincides with a trapped orbit, defined by the separatrix orbit, namely, when $H_t\leqslant H_s$. For $H_t>H_s$, the electron is on an untrapped orbit. Solving $H_t=H_s$ yields in the minimum initial electron momentum for trapping in the plasma wave,[27]

$$u_t=\gamma_\varphi\beta_\varphi(\gamma_\perp-\gamma_\varphi\phi_{\min})-\gamma_\varphi[(\gamma_\perp-\gamma_\varphi\phi_{\min})^2-1]^{1/2}. \tag{7}$$

Equation (7) is valid for a plasma wave potential in a *warm* plasma, where $\phi_{\min}$ is the extrema of the plasma wave potential [solution of Eq. (1)]. Figure 4 shows the initial momentum u_t required for the electron to be trapped by a plasma wave with amplitude $\hat{E}_m=E_{\mathrm{peak}}/E_0$, with $\gamma_\perp=1$. In Fig. 4 the peak electric field corresponding to the minimum potential $\phi_{\min}(\hat{E}_m)$ was solved using Eq. (1) for a warm plasma with $\theta=10^{-4}$. The threshold momentum required for trapping decreases for larger plasma wave amplitude and for lower plasma wave phase velocity. Note that trapping can always occur, even for plasma waves with ultrarelativistic phase velocities ($\beta_\varphi=1$); with $\beta_\varphi=1$ and $\gamma_\perp=1$, Eq. (7) reduces to $u_t=(\phi_{\min}-1/\phi_{\min})/2$.

As shown in Fig. 3(b) (and in Ref. 33) the fields are weakly influenced by the width of the distribution, $E_{\mathrm{peak}}(\theta)/E_0-E_{\mathrm{peak}}(\theta=0)/E_0\sim\theta$, below the wave-breaking limit. Thus, contrary to the claims in Ref. 35, it is an excellent approximation to use the cold fields when studying a warm plasma for typical laser-plasma accelerator parameters. For a cold plasma, the relation between the minimum potential and the field amplitude is

$$\phi_{\min}=\gamma_\perp-1+\hat{E}_m^2/2-\beta_\varphi[(\gamma_\perp+\hat{E}_m^2/2)^2-\gamma_\perp^2]^{1/2}, \tag{8}$$

where $\hat{E}_m=E_{\mathrm{peak}}/E_0$ is the normalized amplitude of the plasma wave field. Equations (7) and (8) can be solved for the peak field E_t required for the onset of particle trapping as a function of the initial electron momentum u_t (Ref. 27),

$$(E_t/E_0)^2\simeq 2\gamma_\perp(\gamma_\varphi-1)+2\gamma_\varphi^2\beta_\varphi\{u_t-[(\beta_\varphi u_t)^2+2\beta_\varphi u_t\gamma_\perp/\gamma_\varphi]^{1/2}\}, \tag{9}$$

where $u_t\ll 1$ (nonrelativistic initial momentum) has been assumed.

Note that trapping occurs in a warm plasma in the ultrarelativistic phase velocity limit where the wave phase velocity is equal to the speed of light $v_\varphi=c$ (as shown in Fig. 4). For $\gamma_\perp=1$, $\beta_\varphi=1$, and $u_t\ll 1$, Eq. (7) yields $\phi_{\min}\simeq -1+u_t$, and, using Eq. (8), the peak field of an ultrarelativistic

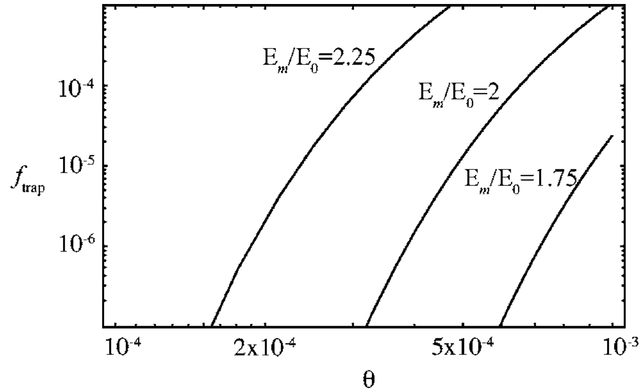

FIG. 5. Fraction of trapped electrons $f_{\rm trap}$ [Eq. (10)] vs the initial temperature of a Gaussian plasma electron distribution $\theta = k_B T_0/mc^2$ for three different nonlinear plasma wave amplitudes driven by a laser with $k_p L_{\rm RMS}=1$ and $a_0=3.65$ ($\hat{E}_m \simeq 1.75$), $a_0=4.15$ ($\hat{E}_m \simeq 2$), and $a_0=4.75$ ($\hat{E}_m \simeq 2.25$), with $\gamma_\varphi=10$.

plasma wave required for trapping an electron with initial momentum u_t is $E_t/E_0 \simeq u_t^{-1/2}$. This result refutes the claim of Ref. 35, that trapping cannot occur for plasma waves with $\beta_\varphi=1$. Indeed, with $\beta_\varphi=1$, the separatrix between trapped and untrapped particles is finite for all phases except ξ_m (which is never reached by a trapped particle).

Equation (7) concerns the trapping in a plasma wave of a single plasma electron with initial momentum u_t. For a thermal plasma electron distribution, electrons on the tail of the distribution function may have sufficiently high momentum so as to reside on trapped orbits. The fraction of electrons trapped in the plasma wave can be computed for a given initial momentum distribution. For example, assuming an initial Gaussian momentum distribution of the plasma electrons with initial temperature T_0 defined by the RMS momentum spread $(k_B T_0/m_e)^{1/2}$, with $(k_B T_0/m_e c^2)^{1/2} \ll 1$ [i.e., a momentum distribution of the form $F(u) \propto \exp(-u^2/2\theta)$], the fraction of trapped electrons is[27]

$$f_{\rm trap} = \frac{1}{2}\,\mathrm{erfc}(u_t/\sqrt{2\theta}), \qquad (10)$$

where u_t is given by Eq. (7). Figure 5 shows the fraction of trapped electrons versus the initial temperature of a Gaussian plasma electron momentum distribution for three different nonlinear plasma wave amplitudes driven by a laser with $k_p L_{\rm RMS}=1$ and $a_0=3.65$ ($\hat{E}_m \simeq 1.75$), $a_0=4.15$ ($\hat{E}_m \simeq 2$), and $a_0=4.75$ ($\hat{E}_m \simeq 2.25$), with $\gamma_\varphi=10$. Note that the plasma wave was calculated assuming a *warm* plasma with temperature θ via Eq. (1). The total number of trapped electrons (i.e., dark current in the plasma accelerator) can be estimated from Eq. (10). For example, for a plasma density of $n_0 = 10^{19}\ \mathrm{cm}^{-3}$, driver transverse size of $r_\perp = 10\ \mu$m, and accelerator length of 1 mm, a trapping fraction of $f_{\rm trap}=10^{-3}$ indicates $\sim$0.1 nC of trapped charge. This trapping calculation neglects beam loading, which implies the wake field induced by the trapped electrons is much smaller than the primary plasma wave, or $n_{\rm trap}/n_0 \ll |\phi|$, where $n_{\rm trap}$ is the density of the trapped electron bunch.

As the driver propagates into the plasma, more charge will be trapped until the amplitude of the plasma wave is substantially reduced due to beam loading. The beam loading limit is defined as the number of accelerated electrons required to produce a wake field that cancels the accelerating field of the plasma wave.[38] The trapped bunch density is approximately given by $n_b \simeq f_{\rm trap} n_0 z/L_b$, where z is the propagation distance and L_b is the bunch length. Assuming $k_p L_b \lesssim 1$, the wake field generated by the bunch is given by $E_b/E_0 \simeq k_p L_b n_b/n_0$ in the 1D limit, assuming $E_b/E_0 < 1$. The beam loading limit at which $E_b \simeq E_m$ is then reached after a propagation distance of $z_{\rm BL} \approx k_p^{-1} f_{\rm trap}^{-1} \hat{E}_m$. For $\hat{E}_m \sim 1$ and $f_{\rm trap} \ll 1$, $k_p z_{\rm BL} \gg 1$ and beam loading will only be significant after long propagation distances.

For a given initial plasma temperature and plasma wave phase velocity, a larger fraction of electrons become trapped as the plasma wave amplitude increases. The particle trapping model presented in this section can be used to calculate the fraction trapped at the hydrodynamic wave-breaking limit. Note that Eq. (9) obtained from trapping theory provides a good estimate to the hydrodynamic wave-breaking field, Eq. (3), over regimes of interest for laser-plasma accelerators, when $u_t = \sqrt{3\theta}$. For example, when $\gamma_\perp=1$, Eq. (7) can be solved for the plasma wave potential required for trapping an electron with initial momentum u_t, i.e., $\phi_{\min} \simeq \gamma_\varphi^{-1} - 1 + \beta_\varphi u_t$, for $u_t \ll 1$; whereas using warm fluid theory, Eq. (2) with $w_z = (1-\chi_0^2)/(1+\chi_0^2)$, the minimum potential at the wave-breaking amplitude is $\phi_{\rm WB} \simeq \gamma_\varphi^{-1} - 1 + \beta_\varphi \sqrt{3\theta}$, assuming $\theta \ll 1$. These two expressions agree when $u_t = \sqrt{3\theta}$. This shows that a significant fraction of the plasma electrons (satisfying $u_t > \sqrt{3\theta}$) can be trapped at the wave-breaking amplitude: $f_{\rm trap} = \mathrm{erfc}(\sqrt{3/2})/2 \simeq 0.04$ for an initial Gaussian momentum distribution. Note that here we have used the potential derived from the *warm* fluid equations. This shows that significant trapping occurs below the wave-breaking limit for a physical initial electron distribution (e.g., Gaussian) and refutes the claim[35] that there is no trapping below the wave-breaking limit.

The warm fluid theory of wave breaking and the trapping calculation assume the quasistatic approximation that the plasma wave is a function of only $\xi = z - v_\varphi t$. In general, for the plasma wave to be a traveling wave that is a function of only ξ implies that there is sufficiently small trapping and beam loading, such that any time-dependent damping of the plasma wave is insignificant (i.e., $k_p z_{\rm BL} \gg 1$, as discussed above). At the wave-breaking amplitude, the fraction trapped is $f_{\rm trap} \simeq 4\%$ assuming an initial Gaussian electron momentum distribution. For example, if the beam loading estimate discussed above is assumed to approximately apply in the nonlinear limit, then $f_{\rm trap} \simeq 4\%$ and $\hat{E}_{\rm WB} \simeq 3$ imply $z_{\rm BL} \simeq 12\lambda_p$. This simple estimation implies that beam loading can lead to appreciable reduction of the plasma wave after several plasma periods if the field amplitude approaches the hydrodynamic wave-breaking limit.

IV. MODELING WITH PARTICLE-IN-CELL CODES

Particle-in-cell (PIC) codes[39–41] have been used extensively to model laser-plasma-based accelerator experiments.

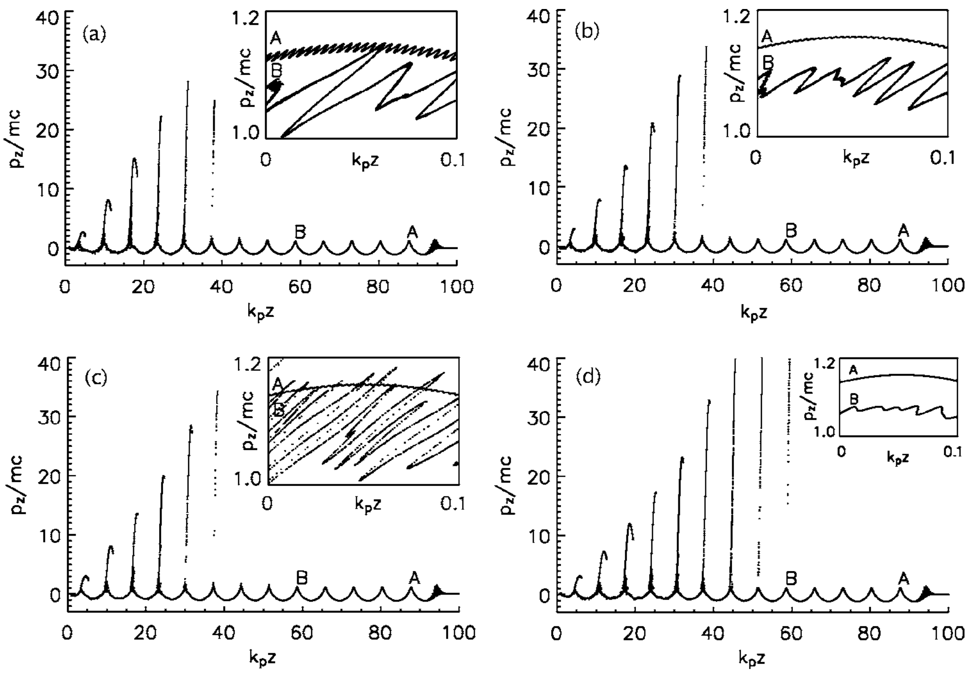

FIG. 6. Macroparticle phase space at $t=15.75\lambda_p/c$, with the physical parameters $\omega_0/\omega_p=10$, $a_0=2$, and $k_pL=2$, using the numerical parameters: (a) $\Delta z=\lambda_0/36$ and $N_{\mathrm{ppc}}=400$, (b) $\Delta z=\lambda_0/48$ and $N_{\mathrm{ppc}}=400$, (c) $\Delta z=\lambda_0/48$ and $N_{\mathrm{ppc}}=100$, and (d) $\Delta z=\lambda_0/48$ and $N_{\mathrm{ppc}}=400$ with a filter (Ref. 47) on the current. The insets show a magnification of the phase space at the first (A) and fifth (B) buckets after the laser pulse.

In a particle-grid approach such as PIC, finite-sized, charged macroparticles interact with electromagnetic fields defined on a grid and interpolated to the macroparticle positions. The unavoidable discretization of the physical model and the small number of macroparticles used to represent the phase-space distribution both give rise to unphysical heating.[40,41] These heating mechanisms include scattering[42] and grid heating.[43] Numerical heating via scattering has a continuous slow growth of momentum spread due to the finite number of macroparticles. The growth of momentum spread depends mainly on the number of macroparticles per cell and on the particle shape. Grid heating[43] has a fast growth rate and saturates when $\lambda_D \sim \Delta z$ in one dimension, where $\lambda_D = (k_B T/4\pi n e^2)^{1/2}$ is the Debye length and Δz the grid size. Interpolation of the gridded field quantities to the macroparticle positions leads to numerical errors in the trajectories that appear to be qualitatively different than the trajectory errors due to truncation in the particle integrator. These numerical errors will alter the macroparticle phase space and can mimic physical processes leading to the incorrect interpretation of computational results. This will be of particular importance when attempting to model detailed kinetic effects, such as trapping of the background electrons or generation of dark current in a plasma-based accelerator.

The effect of the unphysical heating (macroparticle momentum spread) in PIC codes is studied for the case of a nonlinear plasma wave driven by a short laser pulse.[44] For the study described in this section, the initial normalized laser intensity profile is of the form $a_0^2\exp(-2z^2/L^2)$ with $a_0=2$, $k_pL=2$, and $\omega_0/\omega_p=10$. For a 0.8-μm laser wavelength, the plasma wavelength is 8 μm (plasma number density of 1.7×10^{19} cm^{-3}), $L=2.5$ μm (10 fs FWHM laser intensity duration), and peak laser intensity of 8.5×10^{18} W/cm^2. The 1D simulation box is 130 μm long, and the laser was launched from the boundary of the simulation box. The number of grid points varies according to the resolution. The macroparticles are loaded uniformly and cold (no initial momentum), using either $N_{\mathrm{ppc}}=100$ or $N_{\mathrm{ppc}}=400$, where N_{ppc} is the number of macroparticles per cell. For the simulations, a modified version of Plasma Simulation Code (PSC)[45] is used, which implements the standard PIC algorithm[40] and uses a charge-conserving current-deposition scheme.[46]

For this case no self-trapping in the wake is expected because the plasma is initially cold and the wake field is below the cold relativistic wave-breaking field, $E_z < E_0[2(\gamma_\varphi-1)]^{1/2}$. The evolution of the plasma temperature should follow the warm fluid model,[29,33] which predicts that an initially cold collisionless plasma remains cold in this regime. However, the PIC simulations show macroparticles trapped in the wake, as seen in Fig. 6. Figure 6 shows the macroparticle phase space (momentum versus position) at $t=15.75\lambda_p/c$ for the numerical parameters: (a) $\Delta z=\lambda_0/36$ and $N_{\mathrm{ppc}}=400$; (b) $\Delta z=\lambda_0/48$ and $N_{\mathrm{ppc}}=400$; (c) $\Delta z=\lambda_0/48$ and $N_{\mathrm{ppc}}=100$; and (d) $\Delta z=\lambda_0/48$ and $N_{\mathrm{ppc}}=400$ with a (1,2,1) filter (including compensator)[47] on the current. The insets show a magnification of the phase space at the first (A) and fifth (B) buckets after the laser pulse. Note that the wake amplitude is lower in the fifth bucket compared to the first. This is due to the laser evolution (self-steepening of the laser pulse) resulting in a higher peak laser intensity as the laser propagates through the plasma (this has also been confirmed by comparison with 1D cold fluid simulations of the same physical parameters). The insets of Fig. 6 show that, as a function of distance behind the driver, phase space develops an increasingly complex structure. When the plasma current is deposited on the grid, this course graining will yield a current which will have characteristics similar to that due to a warm distribution. In particular this course graining will trigger grid heating, leading to an increasingly large momentum spread. As shown in Figs. 6(a)–6(c), the phase-space structure is dependent on the resolution and number of macroparticles per cell. At a resolution of $\Delta z=\lambda_0/36$ the longi-

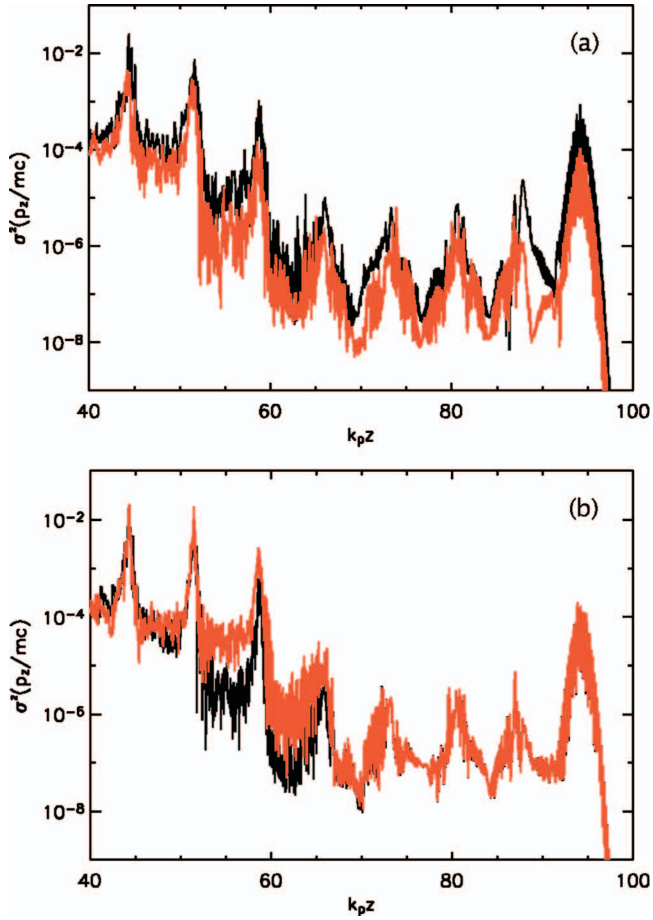

FIG. 7. (Color) (a) Normalized mean-square momentum spread calculated in each cell for $\Delta z=\lambda_0/36$ and $N_{ppc}=400$ (black curve) and $\Delta z=\lambda_0/60$ and $N_{ppc}=400$ (red curve). (b) Normalized mean-square momentum spread calculated in each cell for $\Delta z=\lambda_0/48$ and $N_{ppc}=400$ (black curve) and $\Delta z=\lambda_0/48$ and $N_{ppc}=100$ (red curve). The physical parameters are $\omega_0/\omega_p=10$, $a_0=2$, and $k_pL=2$.

tudinal electric field is accurately represented. Increasing the resolution leads to very little change in the wake field, but results in significant changes in the macroparticle phase space. Note that for a warm initial condition, the PIC algorithm has been shown, with sufficient resolution and macroparticles per cell, to yield the correct thermal plasma response.[33]

The longitudinal mean-square macroparticle momentum spread, $\sigma_u^2=\langle(u-\langle u\rangle)^2\rangle$, is shown in Fig. 7. In this example, secular growth of the momentum spread occurs after the third plasma wave bucket. Increasing longitudinal resolution reduces the momentum spread; Fig. 7(a) shows resolutions of $\Delta z=\lambda_0/60$ (red curve) and $\Delta z=\lambda_0/36$ (black curve). Increasing the macroparticles per cell also reduces the momentum spread; Fig. 7(b) shows $N_{ppc}=100$ (red curve) and $N_{ppc}=400$ (black curve).

V. SUMMARY AND DISCUSSION

The performance of plasma-based accelerators can be affected by finite plasma temperature. Finite temperatures reduce the wave-breaking field and enhance the amount of self-trapped electrons, thus leading to the production of dark current, which will degrade the accelerated electron bunch quality. To correctly determine the temperature evolution, a warm relativistic fluid theory has been derived and analyzed.[29,33] The plasma temperature is found to undergo periodic oscillations in the wake, due to adiabatic compression, but there is no secular heating.[29,33] This is the case since, in the underdense regime of plasma accelerators, there are no collisions, and, in the standard wake-field case, the plasma response is well described using the quasistatic approximation. Using a warm fluid model, an analytical result for the maximum field amplitude of a periodic nonlinear plasma wave (warm wave-breaking limit) was derived.[24] The warm wave-breaking limit, Eq. (3), is capable of describing the regime of current ultraintense short-pulse laser interactions with underdense plasma, in contrast to previous results that are limited to ultrarelativistic particle drive beams. This field amplitude is a fundamental limit on the accelerating gradient in plasma-based accelerators.

For wake amplitudes below the wave-breaking limit, fast particles on the tail of a thermal distribution may become trapped. The trapping of thermal plasma electrons in a nonlinear plasma wave has been examined using a formalism based on single-particle dynamics and the threshold electric-field amplitude for trapping an electron with arbitrary momentum in a nonlinear plasma wave was derived.[27] This calculation included the presence of a laser field, which was found to increase the trapping threshold and, hence, reduce the fraction of trapped electrons. The dark current, or the fraction of electrons trapped, was calculated as a function of initial plasma temperature, wave amplitude, and wave phase velocity.[27]

Several numerical effects in PIC codes can lead to phase-space errors, unphysical heating of the model plasma (i.e., an unphysically large macroparticle momentum spread), and erroneously large levels of particle trapping. Since numerical heating increases with distance behind the wake driver, this issue is worse for larger simulation boxes. For the examples presented in Sec. IV, numerical trapping was observed to occur behind the seventh period of the wake when $a_0=2$. For $a_0=3$, however, numerical trapping occurred after the first three wake periods. Care must be taken in choosing the numerical parameters to ensure that artificial numerical effects are sufficiently small. Although the results presented in this paper have been limited to one dimension, this same general behavior is observed to occur in two–dimensional PIC simulations.[44] Further studies indicate that the use of shaped macroparticles may reduce these effects, however, numerical heating and unphysical trapping will still occur.

ACKNOWLEDGMENTS

The authors would like to thank Hartmut Ruhl for kindly providing the PIC code PSC and for related discussions.

This work was supported by the Office of Science of the U.S. Department of Energy under Contract No. DE-AC02-05CH11231, by the University of Nevada, Reno, under Grant No. DE-FC52-01NV14050, and by a Scientific Discovery through Advanced Computing project, "Advanced Computing for 21st Century Accelerator Science and Technology," which is supported by the U.S. DOE/SC Office of High Energy Physics and the Office of Advanced Scientific Computing Research. This research used the computational resources of an INCITE grant by the U.S. DOE, and of the National Energy Research Scientific Computing Center, which is supported by the Office of Science of the U.S. Department of Energy under Contract No. DE-AC02-05CH11231.

[1] E. Esarey, P. Sprangle, J. Krall, and A. Ting, IEEE Trans. Plasma Sci. **24**, 252 (1996).
[2] A. Modena, Z. Najmudin, A. E. Dangor, C. E. Clayton, K. A. Marsh, C. Joshi, V. Malka, C. B. Darrow, C. Danson, D. Neely *et al.*, Nature (London) **377**, 606 (1995).
[3] R. Wagner, S.-Y. Chen, A. Maksimchuk, and D. Umstadter, Phys. Rev. Lett. **78**, 3125 (1997).
[4] A. Ting, C. I. Moore, K. Krushelnick, C. Manka, E. Esarey, P. Sprangle, R. Hubbard, H. R. Burris, R. Fischer, and M. Baine, Phys. Plasmas **4**, 1889 (1997).
[5] C. Gahn, G. D. Tsakiris, A. Pukhov, J. Meyer-ter-Vehn, G. Pretzler, P. Thirolf, D. Habs, and K. J. Witte, Phys. Rev. Lett. **83**, 4772 (1999).
[6] W. P. Leemans, P. Catravas, E. Esarey, C. G. R. Geddes, C. Toth, R. Trines, C. B. Schroeder, B. A. Shadwick, J. van Tilborg, and J. Faure, Phys. Rev. Lett. **89**, 174802 (2002).
[7] V. Malka, S. Fritzler, E. Lefebvre, M.-M. Aleonard, F. Burgy, J.-P. Chambaret, J.-F. Chemin, K. Krushelnick, G. Malka, S. P. D. Mangles *et al.*, Science **298**, 1596 (2002).
[8] S. P. D. Mangles, C. D. Murphy, Z. Najmudin, A. G. R. Thomas, J. L. Collier, A. E. Dangor, E. J. Divall, P. S. Foster, J. G. Gallacher, C. J. Hooker *et al.*, Nature (London) **431**, 535 (2004).
[9] J. Faure, Y. Glinec, A. Pukhov, S. Kiselev, S. Gordienko, E. Lefebvre, J.-P. Rousseau, F. Burgy, and V. Malka, Nature (London) **431**, 541 (2004).
[10] C. G. R. Geddes, C. Toth, J. van Tilborg, E. Esarey, C. B. Schroeder, D. Bruhwiler, C. Nieter, J. Cary, and W. P. Leemans, Nature (London) **431**, 538 (2004).
[11] W. P. Leemans, B. Nagler, A. J. Gonsalves, C. Tóth, K. Nakamura, C. G. R. Geddes, E. Esarey, C. B. Schroeder, and S. M. Hooker, Nat. Phys. **2**, 696 (2006).
[12] C. G. R. Geddes, C. Tóth, J. van Tilborg, E. Esarey, C. B. Schroeder, D. Bruhwiler, C. Nieter, J. Cary, and W. P. Leemans, Phys. Plasmas **12**, 056709 (2005).
[13] D. Umstadter, J. K. Kim, and E. Dodd, Phys. Rev. Lett. **76**, 2073 (1996).
[14] E. Esarey, R. F. Hubbard, W. P. Leemans, A. Ting, and P. Sprangle, Phys. Rev. Lett. **79**, 2682 (1997).
[15] C. B. Schroeder, P. B. Lee, J. S. Wurtele, E. Esarey, and W. P. Leemans, Phys. Rev. E **59**, 6037 (1999).
[16] G. Fubiani, E. Esarey, C. B. Schroeder, and W. P. Leemans, Phys. Rev. E **70**, 016402 (2004).
[17] H. Kotaki, S. Masuda, M. Kando, J. K. Koga, and K. Nakajima, Phys. Plasmas **11**, 3296 (2004).
[18] J. Faure, C. Rechatin, A. Norlin, A. Lifschitz, Y. Glinec, and V. Malka, Nature (London) **444**, 737 (2006).
[19] A. I. Akhiezer and R. V. Polovin, Zh. Eksp. Teor. Fiz. **30**, 915 (1956), [Sov. Phys. JETP **3**, 696 (1956)].
[20] J. M. Dawson, Phys. Rev. **113**, 383 (1959).
[21] T. P. Coffey, Phys. Fluids **14**, 1402 (1971).
[22] T. Katsouleas and W. B. Mori, Phys. Rev. Lett. **61**, 90 (1988).
[23] J. B. Rosenzweig, Phys. Rev. A **38**, 3634 (1988).
[24] C. B. Schroeder, E. Esarey, and B. A. Shadwick, Phys. Rev. E **72**, 055401 (2005).
[25] C. G. Durfee III, J. Lynch, and H. M. Milchberg, Phys. Rev. E **51**, 2368 (1995).
[26] P. Volfbeyn, E. Esarey, and W. Leemans, Phys. Plasmas **6**, 2269 (1999).
[27] C. B. Schroeder, E. Esarey, B. A. Shadwick, and W. P. Leemans, Phys. Plasmas **13**, 033103 (2006).
[28] S. R. de Groot, W. A. van Leeuwen, and C. G. van Weert, *Relativistic Kinetic Theory* (North-Holland, Amsterdam, 1980).
[29] B. A. Shadwick, G. M. Tarkenton, and E. H. Esarey, Phys. Rev. Lett. **93**, 175002 (2004).
[30] W. A. Newcomb, Phys. Fluids **25**, 846 (1982).
[31] P. Amendt, Phys. Fluids **29**, 1458 (1986).
[32] J. G. Siambis, Phys. Fluids **30**, 896 (1986).
[33] B. A. Shadwick, G. M. Tarkenton, E. H. Esarey, and C. B. Schroeder, Phys. Plasmas **12**, 056710 (2005).
[34] P. Sprangle, E. Esarey, and A. Ting, Phys. Rev. Lett. **64**, 2011 (1990).
[35] R. M. G. M. Trines and P. A. Norreys, Phys. Plasmas **13**, 123102 (2006).
[36] E. Esarey, C. B. Schroeder, W. P. Leemans, and B. Hafizi, Phys. Plasmas **6**, 2262 (1999).
[37] E. Esarey and M. Pilloff, Phys. Plasmas **2**, 1432 (1995).
[38] T. Katsouleas, S. Wilks, P. Chen, J. M. Dawson, and J. J. Su, Part. Accel. **22**, 81 (1987).
[39] J. M. Dawson, Rev. Mod. Phys. **55**, 403 (1983).
[40] C. K. Birdsall, A. B. Langdon, V. Vehedi, and J. P. Verboncoeur, *Plasma Physics via Computer Simulations* (Hilger, Bristol, 1991).
[41] R. Hockney and J. Eastwood, *Computer Simulation Using Particles* (Taylor & Francis, New York, 1988).
[42] R. W. Hockney, J. Comput. Phys. **8**, 19 (1971).
[43] A. B. Langdon, J. Comput. Phys. **6**, 247 (1970).
[44] E. Michel, B. A. Shadwick, C. B. Schroeder, C. G. R. Geddes, E. Esarey, W. P. Leemans, H. Ruhl, and T. Cowan, in *Advanced Accelerator Concepts*, edited by M. Conde and C. Eyberger (AIP, New York, 2006), Vol. 877, pp. 213–219.
[45] H. Ruhl, *Collective Super-Intense Laser-Plasma Interactions* (Habilitationsschrift, Technischen Universität Darmstadt, 2000).
[46] T. Z. Esirkepov, Comput. Phys. Commun. **135**, 144 (2001).
[47] W. B. Mori (private communication).